2019 SECED Conference
Earthquake risk and engineering towards a resilient world
9-10 September 2019, Greenwich, London

CYCLIC MODELLING OF COMPOSITE STEEL-CONCRETE MEMBERS

Burak SAHIN[1], Miguel BRAVO-HARO[2] & Ahmed Y. ELGHAZOULI[3]

***Abstract**: This paper examines the inelastic cyclic behaviour of composite steel-concrete members considering full shear connection. Particular attention is given to the modelling of cyclic deterioration in strength and stiffness in the composite section in the presence of a fully connected concrete slab. Validation is firstly carried out against selected bare steel experimental results using a detailed continuum finite element model, which takes into account both isotropic and kinematic hardening of the steel material. The concrete slab is then added with full shear connection to the steel beam, and modelled using a detailed material model which can simulate the cyclic behaviour of concrete, and is then validated against available experimental results in the literature. The proposed continuum finite element model can satisfactorily simulate the cyclic behaviour of both steel and composite members, and account for the cyclic deterioration in stiffness and strength. The detailed finite element procedure offers a reliable basis for conducting future parametric investigations, with a view to developing design and assessment approaches that incorporate the main cyclic deterioration effects in composite steel-concrete elements.*

Introduction

The use of steel-concrete composite girders has various behavioural and constructional advantages in terms of behavioural and practical aspects compared to bare steel or reinforced concrete counterparts. Composite action increases the flexural stiffness and strength of the steel member and, accordingly, this enables the use of frame systems with larger spans subject to the same loading conditions, amongst other benefits. Therefore, significant research has been carried out on the structural behaviour of composite steel-concrete systems, including on their seismic performance (Elghazouli, et al., 2008).

In order to investigate the behaviour of composite systems consisting of steel beams and reinforced concrete slabs, a number of recent experimental studies were carried out. This included studies with conventional steel beams as well as beams with Reduced Beam Sections (RBS) (e.g., (Nakashima, et al., 2007; Liew, et al., 2000; Doneux & Parung, 2001; Lee, et al., 2016; Ricles, et al., 2004)). However, most of the tests available in the literature were either with low levels of composite action or without shear studs in the expected plastic region of the composite beams (similar to *design concept c* of EC8 (EN 1998-1, 2004), which is discussed in subsequent sections). In addition, only a limited number of these tests used European structural steel section profiles. These limitations in experimental studies on composite sections points to the need for further test assessments, as well as the development of a supplementary numerical database for composite beams and joints by modelling sub-structures through detailed continuum finite elements, as discussed in detail below.

Previous experimental studies showed that: (i) the concrete slab increases the flexural capacity of the steel beam especially under sagging moments; (ii) the moment of inertia of the composite section is significantly larger than that of the bare steel counterpart; (iii) the concrete slab results in unavoidable asymmetric cyclic degradation in stiffness and strength. Additionally, experimental and numerical studies with partial and full shear connection (Bursi, et al., 2005) indicated that composite sections, even with 40% shear connection, could provide the same flexural capacity as fully connected specimens. When the lower design limit of 80% composite action (EN 1994-1, 2004) and reduction factor of 75% for the strength of shear connectors of

[1] PhD student, Imperial College, London, United Kingdom, b.sahin17@imperial.ac.uk
[2] Postdoctoral researcher, Imperial College, London, United Kingdom
[3] Professor, Imperial College, London, United Kingdom

EC8 (EN 1998-1, 2004) are taken into account, composite beams designed according to EC8 imposes a full shear connection (Elghazouli & Castro, 2016). Experimental studies also concluded that as the neutral axis of composite beams is shifted upwards compared to bare steel beams under sagging moments, this leads to higher strain demand at the bottom flange. Accordingly, whilst the top flange of the steel beam restrains the out of plane movement, the bottom flange becomes more susceptible to premature local buckling and fracture. Most of the failure modes of composite specimens involved fracture of the bottom flange.

A number of previous numerical studies focused on modelling of composite steel-concrete beam-slab elements. However, they either examined only a couple of specific parameters, such as moment capacity and slippage between the steel beam and the concrete slab, or were carried out only under monotonic loading (e.g., (El-Lobody & Lam, 2003; Katwal, et al., 2018)). Castro, et al. (2007) investigated the effective slab width of composite beams in the case of full interaction. The steel beam and concrete slab were modelled as beam elements connected using rigid links. However, cyclic degredation phenemona were not considered. More recently, Elkady & Lignos (2014) modelled composite beams by calibrating the modified Ibarra-Medina-Krawinkler (IMK) material model (Ibarra, et al., 2005; Lignos & Krawinkler, 2012) against most of the experimental studies discussed above. Nonetheless, tests without specific classification were used in terms of the level of shear interaction or the type of connection, such as RBS and non-RBS. Their study indicated that the hysteretic cyclic behaviour of a composite beam becomes asymmetric, whilst that of bare steel is symmetric under reversed loads in terms of moment and ductility capacity as well as cyclic degradation in both loading directions. Additionally, El Jisr, et al. (2019) investigated the cyclic behaviour of composite beams by collecting available experiments in the literature. However, as before, the database was mostly composed of non-European steel sections or members without shear studs in dissipative regions, and cyclic degradation phenomena were not investigated.

Effects of Degradation Modelling:

Structures designed according to state of art performance-based seismic design approaches are expected to meet specific and measurable performance requirements. In this respect, reliable estimation of the response of structural systems under realistic seismic excitations is essential. This process necessitates detailed understanding and accurate modelling of the nonlinear cyclic structural response using realistic representation of earthquake ground motion. Therefore, reliable assessment techniques need to be developed taking into account both the structural and ground motion characteristics that can affect the performance. One of the key issues is degradation of structural components in terms of strength and stiffness. Recent investigations (Tsitos, et al., 2018; Bravo-Haro, et al., 2018) on the seismic response of steel moment resisting frames (MRF), taking into account degradation phenomena, showed that both the maximum global and the inter-storey drifts are significantly affected by the degradation of components. According to these studies, structural systems with degradation experienced notably larger deformation demands than non-degrading cases. In addition, incremental dynamic analyses showed that degrading MRFs were more susceptible to the concentration of deformation demands in the lower storeys. Although there are several studies that investigated degradation in steel MRFs, the effects of degradation on seismic response in steel-concrete composite frames have not been examined in detail.

The main objective of this paper is to propose a validated Finite Element (FE) model that can reliably simulate the cyclic behaviour of steel beams acting compositely with a concrete slab by taking into account cyclic strength and stiffness degradation phenomena in both the positive and negative moment directions. This model can then be employed in developing design and assessment approaches that incorporate the main cyclic deterioration effects in composite steel-concrete elements.

Code provisions for composite dissipative elements

The design provisions for composite structures are covered in *Chapter 7* of Part 1 of Eurocode 8 (EC8) (EN 1998-1, 2004), and are mostly based on those for bare steel counterparts, similar to other seismic design codes. There are three main design concepts for composite structures. *Concept a* addresses ductility class low (DCL) as in steel structures. For *Concept a* (DCL), structures may be designed using elastic analysis without taking into account ductile seismic detailing. For the other two concepts, ductility classes medium and high (DCM and DCH, respectively) may be considered with ensuring the fulfilment of ductility and capacity design

requirements. In *Concept b*, dissipative structural behaviour with dissipative composite zones is considered. In the case of *Concept c*, structures are designed with steel dissipative zones, namely no composite action is provided in critical zones. Such structures can be designed according to EC4 (EN 1994-1, 2004) in non-seismic design, and can be considered as steel only in seismic situations. *Concepts a and c* are not within the scope of this paper, and the main focus is on *Concept b* which involves composite dissipative zones.

The behaviour factor q, relates to the reduction adopted in seismic forces in conjunction with the level of ductility demand and energy dissipation required in the structure. EC8 suggests the same upper limits of the behaviour factor, given in Table 6.2 of EC8, for composite regular structural systems, as for steel systems. Additional limiting values are provided in Section 7 of EC8 for composite structures with the combination of steel, concrete or composite shear walls referred to as Structural Types e and f in the code.

Steel beams with concrete slabs:

In EC8, several requirements are given related to ductility, the level of shear connection and the effective width of the slab for steel/concrete composite beams, in order to ensure adequate ductility supply in the critical dissipative zones of structural members. Composite beams can be designed as full or partial shear connected, with a lower limit of 80% shear connection based on previous studies (Bursi, et al., 2005; Bursi & Gramola, 2000). EC8 also requires a 25% reduction of actual resistance of shear connectors. When these two requirements are combined, composite beams a level of shear connection higher than 100% (Elghazouli & Castro, 2016). Therefore, full shear interaction between steel beam and concrete slab is assumed in this research.

To achieve adequate ductility in dissipative zones of composite beams, the strains in the slab under positive bending is required to conform to Eq. (1) as follows:

$$\frac{x}{d} < \frac{\varepsilon_{cu2}}{(\varepsilon_{cu2} + \varepsilon_a)} \tag{1}$$

where x is the distance between top of the concrete slab and the plastic neutral axis; d is the depth of composite section; ε_{cu2} is the ultimate compressive strain of the concrete (EN 1992-1-1, 2004), and ε_a is the total strain in steel at the ultimate limit state (ULS). These parameters are illustrated in Figure 1.

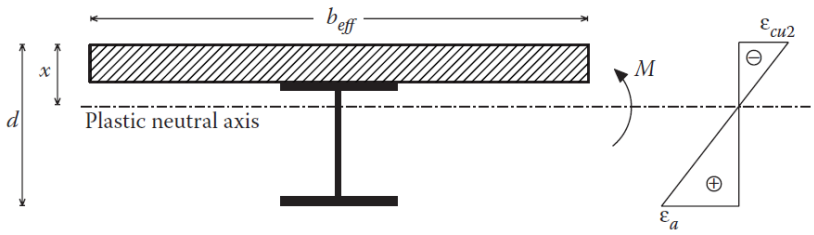

Figure 1. Composite beam section under positive bending (from (Elghazouli & Castro, 2016)).

Another key parameter is the effective width of the concrete slab (b_{eff} from Figure 1), for which EC8 provides two tables (Tables 7.5 I and 7.5 II in the code for elastic and plastic analysis, respectively). The values suggested in those tables depend on various parameters such as the location of the section under consideration, sign of the bending moment, presence of transverse element, dimensions of column, and layout of seismic re-bars. In addition, for non-seismic design situations, EC4 suggests other effective width values. Consequently, designers can be faced with various effective width values. However, previous research conducted by Castro, et al. (2007) showed that the effective width is mostly dependent on the full slab width as well as the thickness of slab, boundary conditions and length of span.

Experimental validation studies

Bare steel beam-column specimens:

Validation studies for the 3D continuum models were firstly performed against tests on bare steel specimens in order to ensure that the recommended model is firstly capable of simulating degradation in steel members. For this purpose, two experimental studies with four different

configurations in total were selected from the literature. For simplicity, experimental studies with fully welded rigid connections were selected herein. The details of those specimens and applied loading protocols can be found in the relevant publications referred to in Table 1.

Popov & Stephen (1972) carried out a series of eight tests on full-scale steel beam-column external connections subjected to cyclic loading with two different beam section sizes and three connection typologies as fully welded, bolted web, and welded flange connection. Only fully welded specimens were modelled as mentioned above. The study concluded that welded connections show higher ductility than bolted cases although all specimens behaved well.

Gilton, et al. (2000) tested five bare steel RBS connection specimens under cyclic loading including two in the weak axis direction. The specimens were designed in order to satisfy strong-column weak-beam ratio of unity as per AISC seismic provisions (AISC, 1997). All beams with strong axis configurations were made of A572 Gr 50 while continuity and doubler plates, if exists, were made of A36 material. Failure modes of the tests were typically twisting of the deep column due to the lateral-torsional buckling of steel beam. In this paper, the specimens with strong axis connection were utilised for validation as in Table 1.

Reference	Spec. Notation	Doubler Plate	Beam	Column	Beam Material
(Popov & Stephen, 1972)	No.2	None	W18x50	W12x106	A36
(Gilton , et al., 2000)	DC1	Yes (10 mm)	W36x150	W27x146	A572 Gr 50
	DC2	None	W36x150	W27x194	A572 Gr 50
	DC3	Yes (16 mm)	W27x194	W27x194	A572 Gr 50

Table 1. Bare steel experimental studies.

Composite beam-column specimens:

For the validation of the FE model of composite beams, experimental studies with full shear connection between the steel beam and concrete slab were employed. For this, the test conducted by Bursi & Gramola (2000) was selected for validation. In this study, six full-scale beam-column specimens were considered with various shear connection levels as full, intermediate, and low with degree of shear connection 1.36, 0.68, and 0.41, respectively. Herein, only the specimen shown in Figure 6, with full shear connection, is used due to limitations discussed before in EC8. IPE 330 and HE360B structural sections were used for the beam and column, respectively. Also, 120 mm reinforced concrete slab with 55 mm steel sheeting with full shear connection to the steel beam as ribs parallel to the beam. The width of the slab was 1200 mm while the length between the column centre line and loading point was 4000 mm, and the distance between pinned support and loading point was 1400 mm. Basic reinforcement was Ø12 with 160 mm and 200 mm spacing in the longitudinal and traverse directions, respectively. Additionally, the reinforcement was doubled in the longitudinal direction at the column region and 2Ø16 were added around the column. The behaviour was governed by the yielding of the bottom flange as well as the reinforcement bars in positive and negative moment, respectively. In addition to the above, a full-scale internal connection specimen with a composite beam tested by Doneux & Parung (2001) was used for the validation of the FE model. Further details of the tests can be found in the above-noted references.

FE Modelling Procedures

Element Types and Mesh Sensitivity Analysis:

In the numerical model, steel beam and column subassemblies were simulated by means of 4-node quadratic “S4R” shell elements that use reduced integration and account for shear deformations. They can also capture local buckling within the cross-section, which is important for degradation modelling. While the concrete slab was modelled as 8-node solid element (C3D8R) with reduced integration and hourglass control, reinforcement bars (linear truss elements, T3D2) were modelled discretely and embedded into the concrete section. Tie constraints were applied between the steel beam and the concrete slab in order to provide full shear interaction by constraining all rotational and translational degrees of freedoms of the nodes on the surface pairs to each other. In this type of constraints, slave and master surfaces need to be determined depending on their rigidity, mesh density, and surface sizes. For example, a stiffer, coarser, and larger surface should act as a master surface, since the program (ABAQUS, 2017) allows master surface penetrate into the slave surface which can

yield to the convergence issues. In this case, the concrete surface acted as master, while the steel part was assumed as slave surface.

In order to determine the most optimal mesh size, a number of buckling and monotonic analyses were carried out for Specimen No.2 (Popov & Stephen, 1972) by reducing the mesh size. The load corresponding to the first buckling mode and the monotonic responses are compared in Figure 2. Buckling analysis was considered in the sensitivity analyses since the mesh size has a notable effect on capturing local buckling, which is critical for characterising the steel component degradation phenomena. Buckling shapes are also given in Figure 3 with related mesh sizes.

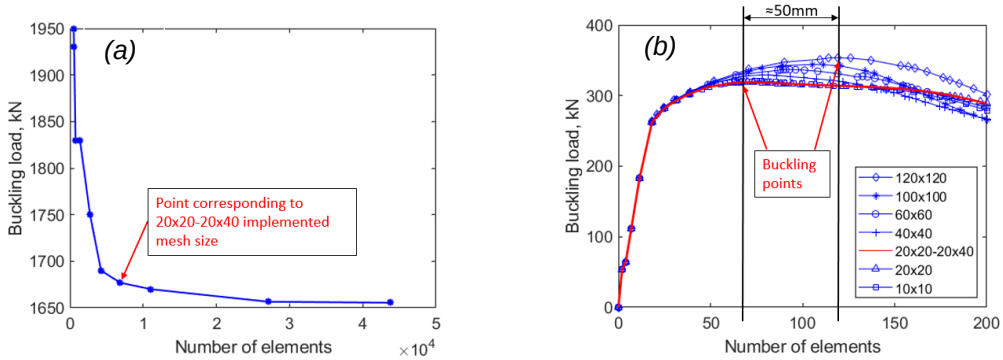

Figure 2. (a) 1st mode linear buckling load vs number of elements, and (b) monotonic response of Specimen No.2 with various mesh sizes.

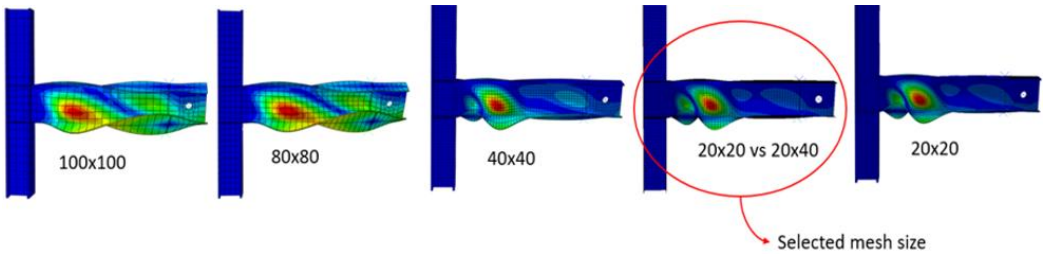

Figure 3. Buckling modes with different mesh sizes for Specimen No.2.

As shown in Figures 2 and 3, for mesh sizes finer than 20mm x 20mm and 20mm x 40mm in expected plasticity and other regions, respectively, the results start to converge. As indicated in the Figure 2a, the first mode Eigen value becomes stable beyond this mesh size. Moreover, the monotonic response indicated in Figure 2b shows that the mesh size has a significant effect on the monotonic response. The differences between the displacements at which buckling occurs is around 50 mm (≈0.02 rad), while the capacity changes approximately by 30 kN (Figure 2b). This discrepancy shows that the buckling displacement can influence significantly the cyclic response of the member since the degradation in the capacity mostly starts after the occurrence of first buckling. Figure 2b shows that for mesh sizes finer than 40x40 mm, the buckling points gets converges at around 70 mm with 330 kN capacity. Additionally, Figure 3 illustrates that the first mode buckling shape of the specimen becomes localised as the mesh becomes finer. As a result of intensive mesh sensitivity analysis and proposed sizes in the literature, 20mm x 20mm and 20mm x 40mm mesh sizes were employed in the regions in which inelasticity is expected (panel zone and beam end) and the other regions, respectively. The mesh size for the solid concrete slab was approximately 140x70 mm along the surface since smaller mesh sizes were increasing the computational time significantly and in some cases lead to numerical instability. The final ABAQUS model used in other studies (Bursi & Gramola, 2000) is also shown in Figure 4 as an example.

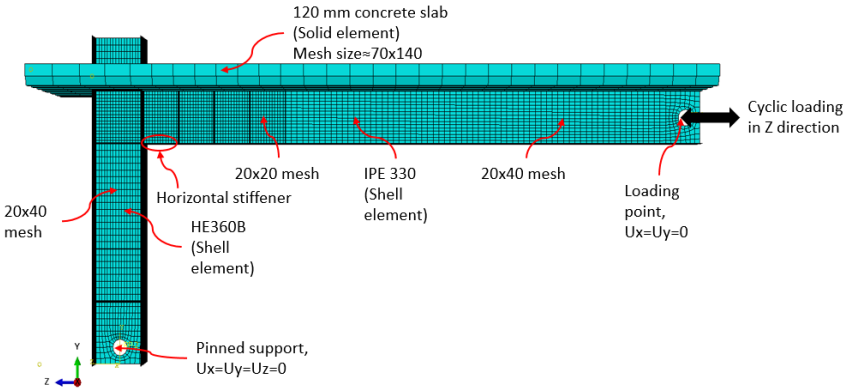

Figure 4. Analytical model of composite specimen (Bursi & Gramola, 2000).

Geometric Imperfections and Residual Stresses:

Geometric imperfections were introduced to take into account typical local instabilities that exist in the specimens within tolerances due to the manufacturing process. Therefore, buckling analyses were carried out prior to the main analyses and superimposition of the most critical buckling modes (see Figure 3) were applied by scaling within the tolerances as discussed in (EN 10034, 1993). In order to obtain the best matching of numerical and experimental results, amplitudes of imperfections were adjusted as they are in the expected range of manufacturing tolerances.

According to previous studies (Elkady, 2016), residual stresses have a negligible influence on the hysteretic behaviour of steel I section beam and columns. Therefore, residual stresses were not considered at this stage in the analyses.

Nonlinear Material Models

Steel members are assigned a combined material model from the ABAQUS material library that takes into account the isotropic/kinematic hardening of the material. The kinematic and isotropic hardening can be defined using Eqs. (2) and (3), respectively.

$$\dot{\alpha} = C\frac{1}{\sigma^{\circ}|_0}(\sigma - \alpha)\dot{\varepsilon}_{pl} - \gamma\alpha\dot{\varepsilon}_{pl} \tag{2}$$

$$\sigma^{\circ} = \sigma^{\circ}|_0 + Q_{\infty}(1 - e^{-b\varepsilon_{pl}}) \tag{3}$$

where C is the initial kinematic hardening modulus, α is the backstress, $\sigma^{\circ}|_0$ is the yield stress at zero plastic strain and can be assumed as F_y, and γ is the rate at which the kinematic hardening modulus, C, decreases with increasing plastic deformation, ε_{pl}. Also, Q_{∞} is the maximum change in the size of the yield surface, and b defines the rate at which the size of the yield surface changes as plastic straining develops. The parameters E, F_y, C, and γ can be obtained from uniaxial coupon tests, Q_{∞}, and b can be extracted from constant amplitude cyclic tests.

The assumed material parameters, as discussed above, are given in Table 2 based on the tests conducted by Krawinkler, et al. (1983) and comply with those used in other studies (Elkady, 2016). The adjustments made in the in material properties were related to the yield stress of the material, which are directly obtained from experimental studies. As for the material model for reinforcement, the isotropic bilinear material model with strain hardening, as suggested in EC2, was employed.

Steel class	C (MPa)	γ	Q_{∞} (MPa)	b
A992 Gr.50 ≈ S355	3378	20	90	12
A36 ≈ S235	6895	25	172	2

Table 2. Isotropic/Kinematic hardening material parameters.

The concrete damage plasticity (CDP) model was utilised for modelling the inelastic behaviour of concrete due to its ability to simulate degradation under cyclic loads. CDP uses the concept of isotropic damaged elasticity with isotropic tensile and compressive plasticity to simulate the inelastic behaviour of concrete. In this study, the compressive behaviour of concrete was

defined from EC2 (EN 1992-1-1, 2004) in the stress-strain domain, while the tensile behaviour of concrete was based on the CEB/FIB model code (CEB/FIB, 2010) in the stress-strain domain in the elastic region and stress-crack opening in the plastic region, as indicated in Figure 5.

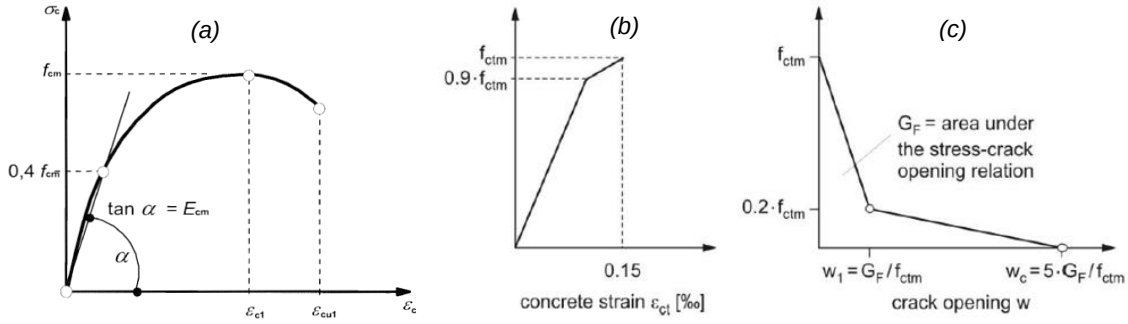

Figure 5. Numerical material model for concrete, a, b, and c are compressive stress-strain, tensile stress-strain, and tensile stress-crack opening graphs, respectively.

Other parameters for CDP such as dilatation angle, eccentricity, the ratio of bi-axial compressive to uniaxial compressive strength, through the K parameter, and viscosity, were assumed as the default values given in ABAQUS, although sensitivity analyses were performed for the dilatation angle and the viscosity parameter. While the computational time decreased remarkably as they increased, degradation in the concrete were more difficult to capture. The stiffness recovery factors for compression and tension were taken as 1 and 0, respectively.The damage parameters required in order to simulate stiffness degradation of concrete were obtained from Eq. (4).

$$d = 1 - \frac{\sigma}{f} \tag{4}$$

It is also assumed that no stiffness degradation occurs before the peak in both the tensile and compressive parts. Where f is the max tensile or compressive strength, as appropriate.

Validation Assessments

Validations of the FE model were firstly performed against bare steel specimens as discussed above. The force vs tip displacement cyclic behaviour of the specimens and the failure modes were compared. As shown in Figure 6a the numerical result is in agreement with the test carried out by Popov & Stephen (1972) in terms of stiffness and capacity. Validation studies for bare steel beam-column specimens were also carried out for the three specimens with reduced beam section (RBS) tested by Gilton, et al. (2000). The results are compared in terms of force vs tip displacement response in Figures 6 b, c, and d. It can be clearly seen that the FEM model is capable of simulating closely the hysteretic behaviour of bare steel beam-column specimens. It can capture the stiffness and capacity, as well as their general degradation trends. Failure shapes for the specimens are not shown herein for compactness.

After obtaining the validated FE model for bare steel specimens, validation studies were performed for the composite specimens. For this purpose, the composite beam/column specimen tested by Bursi & Gramola (2000) and described above was modelled in ABAQUS as discussed earlier, and illustrated in Figure 4. Boundary conditions were assumed as a pinned support at the bottom point of the column and roller support at the loading point. The cyclic displacement loading history was applied in the sliding direction (Z direction) to match that applied in the test. Prior to the main analysis, linear buckling analysis was performed, same as the bare steel specimens, and the critical buckling modes were superimposed and applied to the model in order to take into account geometric imperfections. Realistic implementation of geometric imperfections seemed to be crucial in capturing local buckling accurately in the steel beam, which is one of the main sources of cyclic degradation as mentioned before.

The deformed shape of the specimen at the end of the largest cycle amplitude in the loading history is presented in Figure 7. Buckling in the bottom flange occurs around 250 mm away from the column face due to the presence of a flange 250 mm long and a 12 mm thick flange stiffener. As indicated in the figure, the buckling length was approximately 500 mm and this could be related to the total section depth of 550 mm. This length is expected to affect the

moment-curvature response and, accordingly, the hysteretic behaviour of the member. As shown in Figure 7, the concrete slab prevents the buckling of the top flange and all buckling concentrates in the bottom flange and the bottom side of the web. According to the Von Mises stress values, the top flange is almost in the elastic part whilst yielding and cyclic hardening occurs at the bottom flange and most of the web.

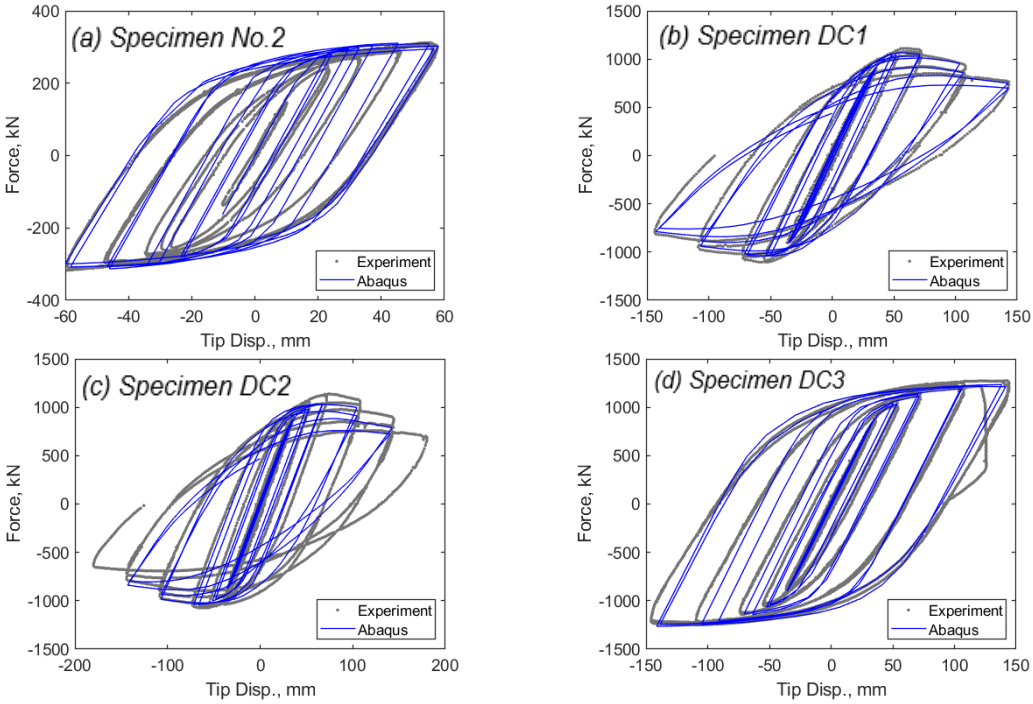

Figure 6. Force vs Tip Displacement graphs for the bare steel specimens.

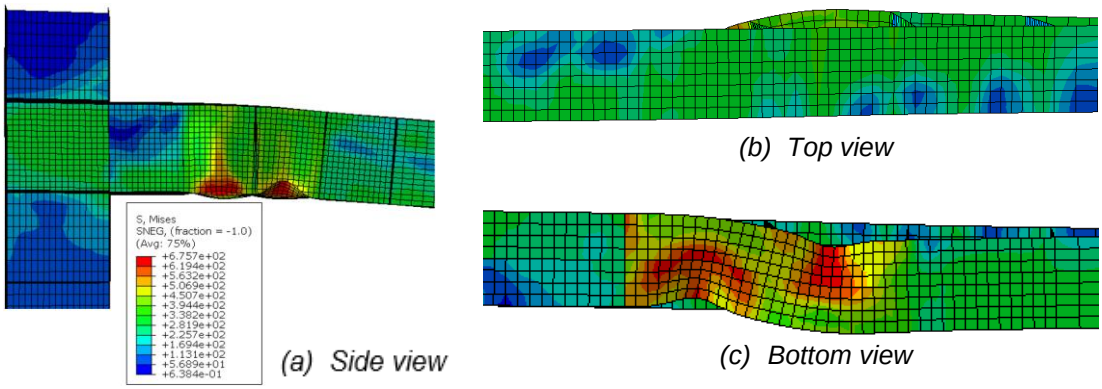

Figure 7. Deformed shapes of the steel part from different views for -100 mm (Push) diplacement amplutide.

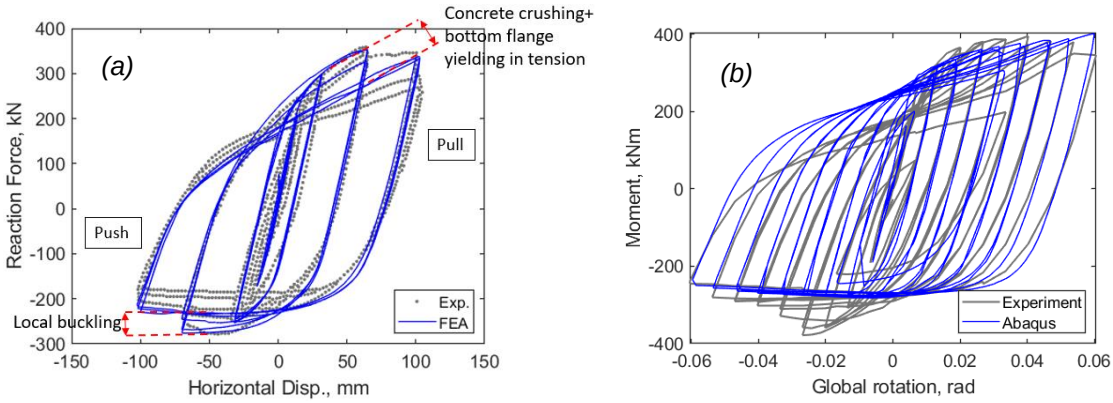

Figure 8. Comparison between experimental and numerical results: (a) (Bursi & Gramola, 2000), and (b) (Doneux & Parung, 2001).

Figures 8a and b show a comparison between the numerical simulation and experimental response for the composite beam specimens (Bursi & Gramola, 2000) and (Doneux & Parung, 2001), respectively. As shown in the figure, the FE model accurately captures most of the parameters, such as stiffness, capacity, and cyclic degradation in both directions. The slight discrepancy in the degradation of capacity in the last few cycles of the loading history is attributed to the cyclic hardening of the steel material as well as the buckling length of the steel part since larger degradation is expected as the buckling length becomes shorter. Although there is no information in the related paper for the full shear connected specimen, for the low partial shear connected specimen the buckling length appears to be approximately 250 mm (Bursi & Gramola, 2000).

Conclusions

This study has investigated the effects of a fully connected concrete slab within a composite steel-concrete member on the cyclic behaviour. Validation studies were firstly carried out on bare steel beam/column sub-assemblages followed by composite steel/concrete configurations, and a refined FE modelling approach for bare steel and composite specimens was proposed.

The FE modelling analysis showed that a faithful implementation of geometric and material nonlinearities is vital for capturing the cyclic degradation in strength and stiffness. As observed from the literature review and the validation studies, the composite action leads to asymmetric behaviour in terms of capacity and ductility in the opposite loading directions, which necessitates more detailed considerations in assessment and design. The flexural strength of composite beams can increase by up to two-fold the strength of bare steel beams. This needs to be considered in capacity design and failure mode control procedures. Moreover, the plastic rotation capacity increases under positive moments (slab is in compression) due to the prevention of local buckling of the top flange due to the restraint from the concrete slab, whilst ductility in the negative direction can decrease compared to bare steel beams due to the increase in strain as a result of the upward shift of the neutral axis. In addition, composite action decelerates the degradation in the positive direction and, accordingly, asymmetric degradation can occur under cyclic behaviour. The detailed finite element procedure offers a reliable basis for conducting future parametric investigations, which are currently underway, with a view to developing design and assessment approaches that incorporate the main cyclic deterioration effects in composite steel-concrete elements, focusing on members designed according to European code provisions.

References

ABAQUS, 2017. *Dassault Systemes Simulia Corp.,* RI, USA: © Dassault Systèmes.

AISC, 1997. *Seismic provisions for structural steel buildings, 2nd Ed.,* Chicago: American Institute of Steel Construction.

Bravo-Haro, M. A., Tsitos, A. & Elghazouli, A. Y., 2018. Drift and rotation demands in steel frames incorporating degradation effects. *Bulletin of Earthquake Engineering,* pp. 1-32.

Bursi, O. S. & Gramola, G., 2000. Behaviour of composite substructures with full and partial shear connection under quasi-static cyclic and pseudo-dynamic displacements. *Materials and Structures,* 33(3), pp. 154-163.

Bursi, O. S., Sun, F.-F. & Postal, S., 2005. Non-linear analysis of steel–concrete composite frames with full and partial shear connection subjected to seismic loads. *Journal of Constructional Steel Research,* 61(1), p. 67–92.

Castro, J. M., Elghazouli, A. Y. & Izzuddin, B. A., 2007. Assessment of effective slab widths in composite beams. *Journal of Constructional Steel Research,* 63(10), p. 1317–1327.

CEB/FIB, 2010. *Model Code 2010-Final draft,* Lausanne, Switzerland: International Federation for Structural Concrete.

Doneux, C. & Parung, H., 2001. DARMSTADT TESTS: A study on composite sub-assemblages. In: A. Plumier & C. Doneux, eds. *Seismic Behaviour and Design of Composite Steel Concrete Structures.* Lisbon: LNEC, pp. 96-106.

El Jisr, H., Elkady, A. & Lignos, D. G., 2019. Composite steel beam database for seismic design and performance assessment of composite-steel moment-resisting frame systems.. *Bulletin of Earthquake Engineering,* pp. 1-25.

Elghazouli, A. Y. & Castro, J. M., 2016. Design of composite steel/concrete structures. In: A. Y. Elghazouli, ed. *Seismic Design of Buildings to Eurocode 8.* s.l.:CRC Press, pp. 193-212.

Elghazouli, A. Y., Castro, J. M. & Izzuddin, B. A., 2008. Seismic performance of composite moment-resisting frames. *Engineering structures,* 30(7), pp. 1802-1819.

Elkady, A., 2016. *Collapse risk assessment of steel moment resisting frames designed with deep wide-flange columns in seismic regions,* s.l.: Doctoral dissertation, McGill University Libraries.

Elkady, A. & Lignos, D. G., 2014. Modeling of the composite action in fully restrained beam-to-column connections: implications in the seismic design and collapse capacity of steel special moment frames. *Earthquake Engineering & Structural Dynamics,* 43(13), pp. 1935-1954.

El-Lobody, E. & Lam, D., 2003. Finite element analysis of steel-concrete composite girders. *Advances in Structural Engineering,* 6(4), pp. 267-281.

EN 10034, 1993. *Structural steel I and H sections-Tolerances on shape and dimensions,* Brussels: European Committee for Standardization.

EN 1992-1-1, 2004. *Eurocode 2: Design of concrete structures - Part 1-1 : General rules and rules for buildings,* Brussels: European Committee for Standardization.

EN 1994-1, 2004. *Eurocode 4: Design of composite steel and concrete structures – Part 1.1: General rules and rules for buildings,* Brussels: European Committee for Standardization.

EN 1998-1, 2004. *Eurocode 8: Design provisions for earthquake resistance of structures, Part 1: General rules, seismic actions and rules for buildings,* Brussels: European Committee for Standardization.

Gilton , C., Chi, B. & Uang, C. M., 2000. *Cyclic response of RBS moment connections: Weak-axis configuration and deep column effects. Rep. No. SAC/BD-00, 23,* San Diego: SAC Joint Venture.

Ibarra, L. F., Medina, R. A. & Krawinkler, H., 2005. Hysteretic models that incorporate strength and stiffness deterioration. *Earthquake engineering & structural dynamics,* 34(12), pp. 1489-1511.

Katwal, U., Tao, Z. & Hassan, M. K., 2018. Finite element modelling of steel-concrete composite beams with profiled steel sheeting. *Journal of Constructional Steel Research,* Volume 146, pp. 1-15.

Krawinkler, H. et al., 1983. *Recommendations for Experimental Studies on the Seismic Behavior of Steel Components and Materials,* Stanford University, California, USA: The John A. Blume Earthquake Engineering Center.

Lee, C. H., Jung, J. H., Kim, S. Y. & Kim, J. J., 2016. Investigation of Composite Slab Effect on Seismic Performance of Steel Moment Connections. *Journal of Constructional Steel Research,* Volume 117, p. 91–100.

Liew, J. R., Teo, T. H., Shanmugam, N. E. & Yu, C. H., 2000. Testing of steel–concrete composite connections and appraisal of results. *Journal of Constructional Steel Research,* 56(2), pp. 117-150.

Lignos, D. G. & Krawinkler, H., 2012. *Sidesway collapse of deteriorating structural systems under seismic excitations,* Stanford, CA: The John A. Blume Earthquake Engineering Center.

Nakashima, M., Matsumiya, T., Suita, K. & Zhou, F., 2007. Full-scale test of composite frame under large cyclic loading. *Journal of Structural Engineering,* 133(2), pp. 297-304.

Popov, E. P. & Stephen, R. M., 1972. *Cyclic loading of full-size steel connections,* s.l.: Center for Cold-Formed Steel Structures Library.

Ricles, J. M., Zhang, X., Fisher, J. W. & Lu, L. W., 2004. Seismic performance of deep column-to-beam welded reduced beam section moment connections. *Connections in Steel Structures V,* pp. 211-221.

Tsitos, A., Bravo-Haro, M. A. & Elghazouli, A. Y., 2018. Influence of deterioration modelling on the seismic response of steel moment frames designed to Eurocode 8. *Engineering & Structural Dynamics,* 47(2), pp. 356-376.